

Hierarchical Control Scheme for Time-Optimal Operation of Semibatch Emulsion Polymerizations

Ralf Gesthuisen,* Stefan Krämer, and Sebastian Engell

Department of Biochemical and Chemical Engineering, Process Control Laboratory, Universität Dortmund, 44221 Dortmund, Germany

A hierarchical control scheme for the time-optimal operation of a semibatch emulsion polymerization reactor using a new technique to calculate the set points of the molar holdups of the reactants is presented and validated by simulations of a rigorous process model. The goal is to produce polymer with a desired molecular weight distribution by emulsion polymerization using a CTA. The novelty of the proposed hierarchical control scheme is that limiting constraints are identified at which the process is operated at its maximum propagation reaction rate. These boundaries result from the avoidance of the formation of a droplet phase and the limited heat removal capacity, the latter of which is an extremely important consideration for larger reactors. To drive the process at its maximum heat removal capacity, a reliable estimation of the heat-transfer coefficient is needed. In the control scheme presented here, a state estimator is used that estimates the heat of reaction and the heat-transfer coefficient of the cooling jacket. Our focus is on the control of pilot-scale and industrial-size reactors; therefore the fact that, for large reactors, the cooling jacket behaves not like an ideal continuously stirred tank reactor (CSTR) but rather like a plug-flow reactor (PFR) must be taken into account. A discretized PDE model of the jacket is used in the estimation scheme. The estimate of the heat of reaction is fed to a simulation model to estimate the amounts of monomer and of CTA in the reactor. The ratio of these two quantities is compared with the required ratio needed to obtain the desired molecular weight distribution, which is calculated off-line. The amount of monomer in the reactor determines the reaction rate, the ratio determines the molecular weight of the polymer obtained. When the process is driven along the constraints, decentralized linear controllers are sufficient to achieve good control performance and to obtain the desired molecular weight distribution.

1. Problem Statement and Proposed Approach

Control of semicontinuous emulsion polymerization processes is an area of active research. Usually, a decomposition approach is applied. In this approach, numerical optimization based on a rigorous model of the process is performed off-line to calculate optimal trajectories. Tracking of the pre-computed trajectory is then realized by on-line feedback control, often employing nonlinear controllers.^{1,2} In most control approaches, model-based measurement techniques such as calorimetry or state estimation are used. In ref 4, the overall heat of reaction in a semibatch emulsion polymerization is determined by calorimetry. Using a simulation model of the process, the conversion and also the concentrations of the monomers in the particle phase are determined in a second step. Master curves are calculated off-line for the total-conversion-dependent amounts of monomer and chain-transfer agent (CTA) that will produce a desired molecular weight distribution when applied in the undisturbed case. Necessary control actions depend on the current estimate of these amounts. Similar control structures have been reported in other publications,^{2–5} although slightly different aspects are included. For example, an extended Kalman filter (EKF) rather than calorimetry is used to estimate the amounts of monomer. Even though some of the authors discuss the influence of parameter uncertainties and plant–

model mismatch and their effect on estimation and control, their control approach can handle these uncertainties and possible disturbances only by using tracking controllers to force the process onto the trajectory calculated off-line.

One of the main parameter uncertainties results from the change in the heat-transfer coefficient during the polymerization process. Especially in optimization-based control strategies, it is important to know the maximum cooling rate, which depends on the heat-transfer coefficient. For on-line optimization, this parameter must be estimated on-line simultaneously with the estimation of the heat of reaction. However, plant–model mismatch can negatively influence the estimation of the heat-transfer coefficient, and because of improper estimator tuning, the estimation of the heat of reaction might also be poor. In this case, a control strategy based on master curves that depend on the estimate must fail.

In this contribution, we propose a novel hierarchical control structure. Only the set points of the ratio of the concentrations of the monomer and CTA are calculated off-line from a desired molecular weight distribution. A decomposition approach where the final molecular weight distribution is produced from ideal instantaneous distributions similar to that described in ref 6 is employed. When the ratio of CTA and monomer for the subsections of the batch are identified, instead of calculating optimal trajectories by numerical optimization, process constraints are analyzed and used to find a time-optimal control strategy, i.e., set points for the total amount of monomer in the reactor are determined

* To whom correspondence should be addressed. E-mail: r.gesthuisen@bci.uni-dortmund.de. Tel.: +49 231 755 5127. Fax: +49 231 755 5129.

at every point of time. The concentrations of the reactants and, in addition, an estimate of the heat-transfer coefficient are required for the on-line application of this concept. Special attention is paid to the effect of the design of the jacket. In pilot-, technical-, or industrial-scale reactors, a jacket usually behaves more like a plug-flow reactor than an ideal continuously stirred tank. Yet, the latter is typically assumed in the literature. We base our estimation of the heat-transfer coefficient on a plug-flow reactor model of the heat transfer to the jacket.

To be able to produce “experimental data” used to check the estimation and control scheme, a simulation model is required. This model is subdivided into an emulsion homopolymerization model with a chain-transfer agent and an energy balance model for the considered equipment.

The paper is organized as follows: In the next section, the simulation model is described. Section 3 presents the hierarchical control approach and the derivation of those constraints on the process that determine the batch time. Section 4 presents the estimation approach. The estimation models, which are simplifications of the simulation models, are also provided. Finally, the hierarchical control approach with the derived estimation method is applied to simulated processes in order to produce an emulsion polymer with a desired molecular weight distribution in minimum process time. Some conclusions are summarized at the end.

2. Process Model

A process model of an emulsion homopolymerization using a chain-transfer agent for molecular weight control is used to produce experimental data of the process. Some of the model equations are also used in the state estimation scheme. This model consists of a kinetic model of the polymerization and a decomposition model of the molecular weight distribution.

The kinetic emulsion polymerization model is based on the following assumptions: (i) monodisperse spherical particles; (ii) constant absolute number of particles N_T (e.g., by use of a seed); (iii) thermodynamic phase equilibrium; (iv) a moderate gel effect that can be fitted by one adjustable parameter; and (v) 0–1 kinetics, i.e., a particle either contains one radical or no radicals corresponding to an average number of radicals per particle of less than 0.5 ($\bar{n} \leq 0.5$).

The last assumption is normally true for styrene emulsion polymerization. Thus, kinetic data for styrene are used. The kinetic model equations used for the simulation can be found in Appendix A.

Additionally, a heat balance model of the jacketed stirred tank reactor is derived in which the jacket is treated as a plug-flow heat exchanger, which is more realistic for large reactors. This model can be found in section 2.1.

To apply the control concept to a real reactor, the simulation model should first be used for controller tuning. The process model has to be adjusted to the real process by fitting the gel effect constant a_1 , the absorption efficiency F_p , and the number of particles N_T . The molecular weight distribution will match a real molecular weight distribution only in a normalized fashion, i.e., only the shape, not the absolute numbers can be compared.

2.1. Energy Balances for a Tubular Jacket. Emulsion polymerizations are usually run in a jacketed

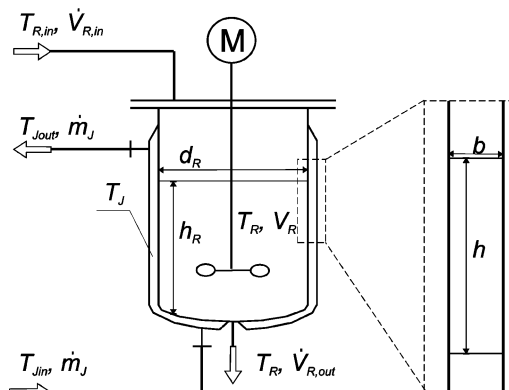


Figure 1. Jacketed reactor.

stirred tank reactor. The jacket is required to heat or cool the reactor contents. There are two main possibilities for modeling of the jacket: For small reactors, possibly immersed in a bath, the jacket behaves like a CSTR. For larger reactors, the jacket, possibly realized as welded-on half pipes, behaves like a plug-flow reactor. Here, we focus on the latter type.

For large reactors, guide plates usually ensure a spiralling flow pattern. The jacket is modeled as a rectangular channel that spirals around the tank. The spiralling effect is neglected. We assume that the channel is a rectangular pipe, perfectly insulated on three sides and contacting the reactor wall on one side. Its length is L , its width is b , and its height is h .

If the reactor is not completely filled, no heat is exchanged between the reactor and jacket in the upper part of the vessel, as the heat transfer from the gaseous phase to the jacket is negligible compared to that from the liquid phase to the jacket. Therefore, this upper part is modeled separately just considering the convective term, which means it is simply a time delay.

The heat balance for the reactor contents reads

$$\frac{d[C_S(T_R - T_{\text{ref}})]}{dt} = r_M^p V^p (-\Delta H) - \dot{Q}_J + \dot{n}_M M_M c_{pM} (T_{R,\text{in}} - T_{\text{ref}}) + \dot{n}_X M_X c_{pX} (T_{R,\text{in}} - T_{\text{ref}}) + \dot{V}_W \rho_W c_{pW} (T_{R,\text{in}} - T_{\text{ref}}) \quad (1)$$

$$C_S = \sum_{i \in \{M, X\}} n_i M_i c_{pi} + V_{\text{Pol}} c_{p\text{Pol}} \rho_{\text{Pol}} + V_{\text{WC}} c_{p\text{WC}} \rho_{\text{WC}} + C_{\text{equip}} \quad (2)$$

$$A = \frac{\pi}{4} d_R^2 + \pi d_R h_R \quad (3)$$

where T_R and T_J are the reactor and jacket temperatures, respectively; $(-\Delta H)$ is the heat of reaction; k is the heat-transfer coefficient; A is the heat-transfer area; M_i , c_{pi} , and ρ_i are the molecular weight, heat capacity, and density, respectively, of species i ; $T_{R,\text{in}}$ is the temperature of the feed streams; C_{equip} describes the heat capacity of the equipment; d_R is the diameter of the tank; and h_R the height of liquid in the tank. T_{ref} is the reference temperature for the heat capacities and can be omitted without loss of generality.

Most of these symbols are also depicted in the schematic drawing of a jacketed reactor (Figure 1). The heat of reaction of the CTA reaction is not considered,

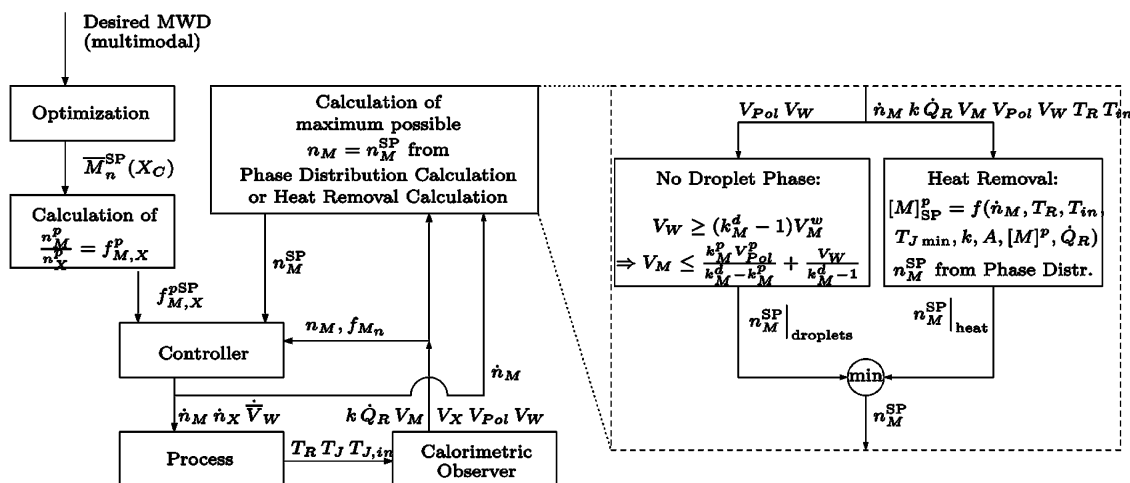


Figure 2. Description and explanation of the hierarchical control concept.

as the CTA reaction rate is several orders of magnitude smaller than the propagation rate.

The lower jacket is modeled by a first-order partial differential equation, where the axial dispersion is neglected, i.e., an ideal plug-flow behavior is assumed

$$\frac{\partial T_{J,L}(z)}{\partial t} = -v_J \frac{\partial T_{J,L}(z)}{\partial z} + \frac{k}{b\rho_J c_{pJ}} [T_R - T_{J,L}(z)] \quad (4)$$

Here, $T_{J,L}(z)$ is the temperature distribution depending on the spatial coordinate z in the lower part of the jacket along the uncoiled spiral channel; z is the spatial coordinate; and v_J is the cooling or heating fluid velocity, which can be calculated by

$$v_J = \frac{\dot{m}_J}{\rho_J b h} \quad (5)$$

where \dot{m}_J is the jacket flow rate of the cooling or heating medium and c_{pJ} is its heat capacity. $T_{J,in}$ is the inlet temperature of the cooling or heating medium. In the upper part of the jacket, heat transfer is neglected. This gives the following equation

$$\frac{\partial T_{J,U}(z)}{\partial t} = -v_J \frac{\partial T_{J,U}(z)}{\partial z} \quad (6)$$

Here, $T_{J,U}(z)$ is the temperature distribution in the upper part of the jacket. The channel is spiralling around the reactor. The area covered with liquid is given by eq 3 and remains the same. The area A_{\max} is the maximum heat-transfer area covered by the jacket corresponding to $h_{R,\max}$. The assumed rectangular channel has to cover both of these areas. Thus, the length of the channel up to the liquid level and the maximum length can be identified as

$$L = \frac{A}{h_R} \quad (7)$$

$$L_{\max} = \frac{A_{\max}}{h_{R,\max}} \quad (8)$$

where the length of the upper part of the jacket is then given by $L_{\max} - L$.

The manipulated variable for the jacket is $T_{J,in}$. For the lower part of the jacket, the manipulated variable

is the boundary condition of eq 4. \dot{Q}_J is found by integrating the heat transfer over every area element dz up to length L

$$\text{boundary} \quad T_{J,L}(0, t) = T_{J,in}(t) \quad (9)$$

$$\text{heat flow} \quad \dot{Q}_J = \int_0^L kh [T_R - T_{J,L}(z)] dz \quad (10)$$

where h denotes the height of the channel. For the upper part of the jacket, the boundary condition is given by

$$T_{J,L}(L, t) = T_{J,U}(0, t) \quad (11)$$

Equations 4 and 6 approximately describe the “true” behavior of the jacket for large reactors.

2.2. Model Summary. A model of the simulation of a homopolymerization using a CTA to influence the chain length distribution has been provided (Appendix A). The model assumes a constant number of particles and contains three adjustable parameters. The model is complemented by an energy balance to model the evolution of the temperature in the vessel and in the cooling jacket. The energy balance considers the jacket as a plug-flow reactor (PFR).

3. Hierarchical Control Approach

In this section, we present a hierarchical, time-optimal control concept for the class of processes described by the model in section 2 and Appendix A. The goal is to produce a desired molecular weight distribution in minimal time. This is done by operating the process along one of two limiting constraints, the maximum heat removal or the avoidance of a droplet phase, both of which describe the case of a maximum heat of reaction and thus a minimum process time.

Figure 2 shows the hierarchical control concept in block diagram fashion. It consists of the following steps:

1. The desired molecular weight distribution of the final product is specified by the operator.

2. This desired MWD is decomposed into the average molecular weights that have to be produced in certain conversion intervals. This computation is labeled “Optimization” in Figure 2. The computation is performed off-line using a method similar to the one presented in ref 6. A detailed explanation can be found below in section 3.1. The result of the optimization is a series of conversion sections in which polymer with a specified

average molecular weight (\bar{M}_n^{SP}) needs to be produced. The production of this average molecular weight is possible using a specified ratio between the amounts of monomer and CTA in the particle phase ($f_{M,X}^{\text{P}}$), which is used to calculate the feed rate of CTA during the process.

3. During the course of the reaction, the set-point trajectory of the molar monomer holdup in the reactor is calculated on the basis of the estimated amount of monomer in the reactor and the conditions that no droplet phase should be present and that the maximum heat removal capacity should not be exceeded. This calculation is labeled "Calculation of maximum possible n_M ..." in Figure 2. Calculation details are given below in section 3.2.

4. Using $f_{M,X}^{\text{P}}$ and n_M^{SP} , the set points for the amounts of monomer and CTA in the reactor are calculated using the phase distribution calculation. Details are given in section 3.3.

5. The true amounts of monomer and CTA in the reactor are estimated using a calorimetric observer, and the ratio between the total molar holdups of monomer and CTA for the desired average molecular weights in the intervals are calculated. The estimation details are provided below in section 4.

6. Using the calculated set points and the estimated true values, the required control actions are calculated. The controller design is given in section 3.4.

Similar hierarchical control strategies have already been proposed by other authors (e.g., ref 4). The novelty of the approach proposed here is the on-line calculation of the set points of the holdups of monomer and CTA. If the time-optimal solution of the semibatch process is analyzed, it turns out that this solution is characterized by the operation at certain constraints. These constraints, which result in nonlinear inequality constraints in the nonlinear dynamic optimization problem used, for example, in ref 7, are the avoidance of the formation of a droplet phase and the limited heat removal capacity of the reactor. Both affect the maximum allowed reaction rate. Therefore, the main difference from other existing approaches lies in step 3.

3.1. Calculation of the Average Molecular Weights. If the termination reaction is dominated by a chain-transfer agent, the MWD of linear polymers formed in an ideal polymerization can be described by the combination of ideal MWDs (Schulz–Zimm distributions) with specific average molecular weights.^{1,6,8} For process operation, each of these contributions can be assigned a certain part of the total conversion to provide the total molecular weight distribution. These intervals can be found by optimization.⁶ The free parameters in this optimization step are the average molecular weights of the different modes and the fractions of the total conversion for which these molecular weights are produced. Given a desired MWD and a number of modes, the fractions of conversion and the corresponding average molecular weights can be determined by a least-squares approach

$$\min_{M_{n,j}, X_{C,j}} \Phi = [\bar{W}_{\text{given}}(n) - \bar{W}(n)]^2 \quad (12)$$

$$\text{s.t.} \quad \bar{W}(n) = \sum_j (X_{C,j} - X_{C,j-1}) \frac{n}{\bar{M}_{n,j}^2} \exp\left(-\frac{n}{\bar{M}_{n,j}}\right) \quad (13)$$

If the specified number of modes is not sufficient to

represent the desired MWD, it should be increased, and the optimization must then be repeated.

This approach is only applicable for "low conversion and polymer made to have a certain molecular weight" and for termination by disproportionation or chain transfer, where the polydispersity index is 2 (ref 9, p 68). These conditions are fulfilled for the instantaneous molecular weight distribution using CTA as the main termination event.¹ They need to be fulfilled only for the instantaneous MWD, as the final MWD is the integral of the instantaneous MWD over the conversion. For the polymerization of styrene used as an example here, numerical conditions have been derived under which the termination of radical chains in an emulsion polymerization with CTA is dominated by the chain-transfer reaction and therefore by the ratio between the monomer concentration and the CTA concentration in the particle phase. In this case, the instantaneous number-average molecular weight is calculated by

$$\bar{M}_n = \frac{k_p[M]^{\text{P}}}{k_{f,X}[X]^{\text{P}}} M_M \quad (14)$$

where M_M denotes the molecular weight of the monomer. For styrene, this equation holds for the following conditions¹

$$\frac{[X]^{\text{P}}}{[M]^{\text{P}}} > 5.2 \times 10^{-6} \quad [X]^{\text{P}} > 3.5 \times 10^{-6} \quad (15)$$

3.2. Set-Point Calculation. As indicated in Figure 2, two conditions are evaluated to determine the maximum reaction rate, i.e., the largest possible concentration of monomer in the particle phase. These two conditions are (i) a droplet phase should not be present and (ii) the reaction rate must not exceed the maximum heat removal capacity.

The latter condition is often neglected in trajectory optimization of emulsion polymerization reactors. If laboratory-scale reactors ($V_R \leq 1$ L) are considered, this condition does not limit the reaction rate because of the high surface-to-volume ratio and high flow rates of the cooling medium and the resulting high cooling capacity. For pilot-scale or larger reactors, this criterion becomes increasingly important.

As a result of these two calculations, maximum numbers of moles of monomer in the reactor are calculated, the minimum of which is used as the set point of the controller. Below, algebraic relations are derived that are used for the on-line calculation of the desired molar holdup of each reactant.

3.2.1. Avoiding a Droplet Phase. When the maximum swelling of the polymer particles with monomer is exceeded, a monomer droplet phase will form alongside the water and particulate phases. The droplet phase cannot increase the reaction rate, as the reaction rate in the polymer particles depends solely on the amount of monomer in the particles. This amount cannot be increased by adding monomer, which will only accumulate in the droplet phase.

A droplet phase will result in poor controllability of the process, as the reaction rate cannot be changed from the outside until the droplets are depleted. This makes temperature control more difficult, as a monomer reservoir accumulates that is emptied only by the

reaction. Hence, a droplet phase is unnecessary and potentially dangerous and should be avoided.

Because of the small amount of CTA present in the reactor, it can be assumed that the CTA has no strong influence on the phase distribution of the monomer. To account for this and other uncertainties, a safety margin for the maximum amount of monomer is introduced. The system is therefore treated as a homopolymerization.

A droplet phase will form if the water phase is saturated with monomer. From eqs 80–85 below, the following condition for the nonexistence of a droplet phase can be derived¹⁰

$$V_W \geq (k_M^d - 1)V_M^w \quad (16)$$

where V_W is the amount of water in the reactor, k_M^d is the partition coefficient between the droplet and the water phase, and V_M^w is the volume of monomer dissolved in the water phase.

To calculate the maximum total amount of monomer allowed in the system to avoid the formation of a droplet phase, the amount of water and the amount of polymer in the particles need to be known. Here, V_{Pol} and V_W are estimated (see below, section 4). The maximum amount of monomer can now be calculated using the following equations and inequality 16 as

$$k_M^p \frac{V_M^w}{V^w} = \frac{V_M^p}{V^p} \quad (17)$$

$$V^w = V_M^w + V_W \quad (18)$$

$$V^p = V_M^p + V_{Pol} \quad (19)$$

$$V_M = V_M^p + V_M^w \quad (20)$$

Combining these equations, the upper bound of the set point of the molar holdup, n_M^{SP} , results

$$n_M^{SP} = \left(\frac{k_M^p V_{Pol}}{k_M^d - k_M^p} + \frac{V_W}{k_M^d - 1} \right) V_M \varphi \quad (21)$$

Here, $\varphi < 1$ denotes the safety margin. With increasing conversion, i.e., with increasing amount of polymer, the maximum amount of monomer calculated from eq 21 will increase, as it depends on the swelling of the polymer. In contrast, the heat removal capacity decreases, as the heat-transfer coefficient decreases significantly with increasing solids content. Thus, in reactors of larger scale, the limited heat removal capacity will restrict the acceptable amount of free monomer once a certain amount of polymer is present in the system.

3.2.2. Maximum Heat Removal. In the calculation of the heat of reaction, only the propagation reaction is considered as it provides the main contribution to the total heat of reaction. This reaction rate is given by eq 62 below. The heat of reaction can be expressed as

$$\begin{aligned} \dot{Q}_R &= r_M^p(-\Delta H) \\ \dot{Q}_R &= k_p[M]^p \frac{N_T}{N_A V^p}(-\Delta H) \\ \Leftrightarrow \frac{\bar{n}N_T}{N_A V^p} &= \frac{\dot{Q}_R}{k_p[M]^p(-\Delta H)} \quad (22) \end{aligned}$$

The maximum heat removal is achieved when the jacket inlet temperature is at its minimum ($T_{J,in,min}$) or slightly above this value so that the temperature controller can still react to disturbances. The aim of time-optimal control is achieved if the reactor is isothermally operated at this constraint.

For isothermal operation, the heat balance in the reactor reduces to

$$\frac{dC_S}{dt}T_R = \dot{V}_{in}\rho_{in}c_{p,in}T_{in} - \dot{Q}_J + \dot{Q}_R \quad (23)$$

The stationary solution of eq 4 for $z = L$ and $T_J(z = 0) = T_{J,in,min}$ yields

$$T_{J,out} = T_R - (T_R - T_{J,in,min}) \exp\left(-\frac{k}{b\rho_J c_{p_J} v_J}L\right) \quad (24)$$

$\dot{Q}_{J,max}$ can now be calculated by inserting eq 24 into eq 10 and integrating to obtain

$$\begin{aligned} \dot{Q}_{J,max} &= \int_0^L kh(T_R - T_{J,in,min}) \exp\left(-\frac{k}{b\rho_J c_{p_J} v_J}x\right) dx \\ &= c_p \dot{m}_j (T_R - T_{J,in,min}) \left[1 - \exp\left(-\frac{kA}{c_p \dot{m}_j}\right) \right] \quad (25) \end{aligned}$$

which is the same result as is obtained by using eq 24 in the log mean temperature difference.

If it is assumed that dC_S/dt depends only on the input flow rate of the reactor, then the maximum heat of reaction is calculated by

$$\dot{Q}_{R,max} = k_p[M]_{max}^p \frac{\bar{n}N_T}{N_A V^p}(-\Delta H) = [M]_{max}^p \frac{\dot{Q}_R}{[M]^p} \quad (26)$$

Assuming that $dC_S/dt = \dot{V}_{in}\rho_{in}c_{p,in} = \dot{V}_{in}\rho c_p$ and inserting the current heat of reaction into this relation, eq 23 can be written as

$$\dot{V}_{in}\rho c_p(T_R - T_{in}) = -\dot{Q}_{J,max} + \frac{[M]_{max}^p}{[M]^p} \dot{Q}_R \quad (27)$$

leading to the following solution for the maximum concentration of monomer in the particle phase $[M]_{max}^p$

$$[M]_{max}^p = \left[\dot{V}_{in}\rho c_p(T_R - T_{in}) + \dot{Q}_{J,max} \right] \frac{[M]^p}{\dot{Q}_R} \quad (27a)$$

By adjusting $T_{J,in,min}$, a safety margin can be defined. The bound on n_M^{SP} can now be calculated from the inverse of the phase distribution calculation.

For a monomer with very low water solubility, it can be assumed that no phase distribution is necessary, yielding the following simple result

$$n_M^{SP} = [M]_{\max} \frac{V_{Pol}}{1 - [M]_{\max}^p V_M} \quad (28)$$

3.3. Calculation of the Total Molar Holdup Ratio.

The off-line calculation of step 2 gives the ratio $f_{M,X}^p$ between monomer and CTA in the polymer particle phase. As the controlled variables are the total amounts of the reactants, the desired ratio of these values must be determined. Hence, the phase distribution algorithm¹¹ has to be reformulated and extended by the following equation

$$V_X = \frac{V_X V_M}{V_M f_{M,X}} \frac{1 + \frac{V^w}{V^p k_X^p} + \frac{V^d k_X^d}{V^p k_X^p}}{1 + \frac{V^w}{V^p k_M^p} + \frac{V^d k_M^d}{V^p k_M^p}} \quad (29)$$

Through the introduction of this equation, the amount of CTA in the particle phase becomes dependent on the total amount of CTA in the reactor, now a free variable. From the solution of the modified phase distribution algorithm, the desired ratio is given by

$$f_{M,X} = \frac{V_M V_X}{V_X V_M} \quad (30)$$

where V_X and V_M denote the molar volumes of the CTA and of the monomer, respectively.

Figure 3 shows the dependency of the ratio $f_{M,X}$ on the volumes of the polymer and monomer. The desired ratio in the polymer is $f_{M,X}^p = 3 \times 10^5$. It follows that, for a wide range of polymer and monomer volumes, the two ratios (particle and reactor) are nearly identical. If a droplet phase exists, the necessary ratio of the molar holdups of monomer and CTA in the reactor differs significantly from the desired ratio in the particle phase. The set point of the total molar holdup reads

$$n_X^{SP} = \frac{n_M^{SP}}{f_{M,X}} \quad (31)$$

3.4. Controller Design. The calculations above result in a time-optimal set-point trajectory of the process performed at its constraints.¹² In this section, the design of the controller that tracks the calculated trajectory is briefly discussed.

In simulation experiments, it was found that simple decentralized PI controllers are sufficient to control the molar holdups.

In general, emulsion polymerization processes are highly nonlinear. Because the formation of a droplet phase is being avoided and because monomer and CTA do not interact significantly, the nonlinearities exist only in the phase distribution calculation. Therefore, it is possible to apply linear decentralized controllers to track the set points of the molar holdups of monomer and CTA. The gains of the controllers were adjusted by simulation studies.

3.5. Summary. The hierarchical control concept shown in Figure 2 provides the set points (n_X^{SP} and n_M^{SP}) along the constraints for time-optimal control. Either the avoidance of a droplet phase or the maximum heat removal is used as a constraint. To calculate these set points on-line, actual process data are needed. Upon

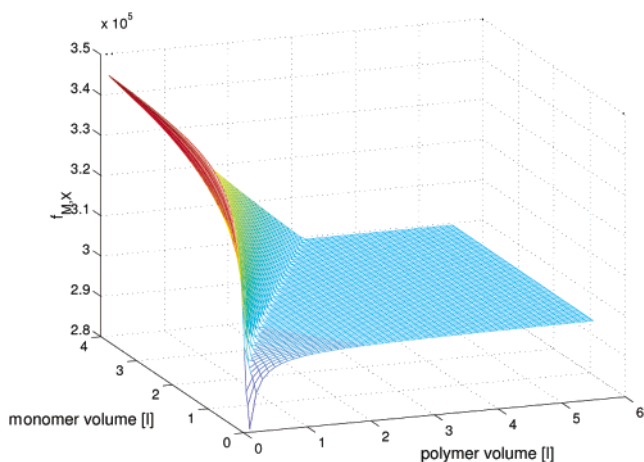


Figure 3. Dependency of $f_{M,X}$ on the volumes of the polymer and monomer.

recapitulation of the above equations, the following process variables for the control concept are found to be required: (i) n_M , the current overall amount of monomer in the reactor, which is determined from \dot{Q}_R , the current heat of reaction; (ii) k , the current overall heat-transfer coefficient; (iii) n_X , the current overall amount of CTA in the reactor; (iv) V_{Pol} , the current volume of polymer in the reactor; and (v) V_W , the current amount of water in the reactor. Apart from V_W , which is known because water is assumed not to participate in this polymerization reaction, these process variables have to be measured or estimated during a batch run.

4. State Estimation

To calculate all of the above process variables, a stepwise state estimation procedure, which is also called "open-loop state estimation",¹³⁻¹⁵ is applied. In this approach, the heat of reaction is estimated using calorimetry. The heat of reaction is used in a kinetic model that is simulated in parallel to the process and thus provides the desired states.

In our control approach, estimates of the heat of reaction and of the heat-transfer coefficient are needed. We propose an extended Kalman filter¹⁶ (EKF) instead of a heat balance calorimetry to estimate \dot{Q}_R and k simultaneously.¹⁷ This approach is suitable for large reactors (>10 L) and complementary to oscillation calorimetry,¹⁸ which is suitable for small reactors (<10 L). Oscillation calorimetry can be used for small reactors with high jacket flow rates and possibly fails for low jacket flow rates and large reactors. The EKF, however, works better with larger reactors and lower mass flow rates through the jacket, such as those encountered in the reactor configuration investigated here.

The proposed strategy is as follows: The heat balance model, assuming either a well-mixed jacket or a tubular jacket, is used in the EKF. The values \dot{Q}_R and k are added as parameters and estimated. k is used directly in the control scheme. \dot{Q}_R is used to calculate the set point for the molar holdup of the monomer and in the dynamic model of the process to find the missing parameters n_M , the overall amount of monomer in the reactor; n_X , the overall amount of CTA in the reactor; V_{Pol} , the volume of polymer in the reactor; and V_W , the amount of water in the reactor.

In this section, the EKF is first explained. Afterward, model adjustments for use in the EKF are provided. Finally, the use of \dot{Q}_R in the simulation model is explained.

4.1. EKF Implementation. Rigorous modeling of dynamic systems usually yields nonlinear differential equations of the form

$$\begin{aligned}\dot{\mathbf{x}} &= \mathbf{f}(\mathbf{x}, \mathbf{u}) + \xi(t) \\ \mathbf{x}(0) &= \mathbf{x}_0 + \xi_0\end{aligned}\quad (32)$$

$$\mathbf{y}(t) = \mathbf{h}(x) + \varphi(t) \quad (33)$$

where \mathbf{x} , \mathbf{u} , \mathbf{y} , ξ , and φ are the n -dimensional state vector, the r -dimensional vector of control variables, the m -dimensional measurement vector, the n -dimensional vector of the model errors, and the m -dimensional vector of the measurement errors, respectively. The EKF is one of the most frequently applied state estimation techniques in chemical engineering. It assumes that ξ and φ represent zero-mean normally distributed random processes.

In technical applications, sampled systems are considered. Hence, the ordinary differential equations have to be transformed into difference equations by integration over one sampling interval

$$\begin{aligned}\mathbf{x}_{k+1} &= \mathbf{x}_k + \int_{t_k}^{t_{k+1}} \mathbf{f}(\mathbf{x}, \mathbf{u}) + \xi_k dt \\ &= \mathbf{F}(\mathbf{x}_k, \mathbf{u}_k) + \xi_k, \quad \xi_k \sim \mathcal{N}(0, \mathbf{Q})\end{aligned}\quad (34)$$

$$\mathbf{y}_k = \mathbf{h}(\mathbf{x}_k) + \varphi_k, \quad \varphi_k \sim \mathcal{N}(0, \mathbf{R}) \quad (35)$$

The discrete linear Kalman filter is based on the solution of the minimization of the expected values of the estimation error for linear dynamics and thus provides optimal estimates for the given covariance matrices. The covariance matrices \mathbf{Q} and \mathbf{R} usually are not known but can be considered as weighting matrices of the estimation errors. The solution of this optimization problem requires the solution of the matrix Riccati equation.¹⁶

The extended Kalman filter is an extension of the linear Kalman filter for nonlinear dynamics. The linear model equations in the prediction part are replaced by the nonlinear process model, and the prediction of the covariance matrix of the estimation error $\mathbf{P}_{k+1|k}$ is performed by Taylor linearizing the process model. The filter equations result as follows

Correction terms

$$\hat{\mathbf{x}}_{k|k} = \hat{\mathbf{x}}_{k|k-1} + \mathbf{K}_k [\mathbf{y}_k - \mathbf{h}(\hat{\mathbf{x}}_{k|k-1})] \quad (36)$$

$$\mathbf{K}_k = \mathbf{P}_{k|k-1} \mathbf{H}_{k|k-1}^T (\mathbf{H}_{k|k-1} \mathbf{P}_{k|k-1} \mathbf{H}_{k|k-1}^T + \mathbf{R})^{-1} \quad (37)$$

$$\mathbf{P}_{k|k} = (\mathbf{I} - \mathbf{K}_k \mathbf{H}_{k|k-1}) \mathbf{P}_{k|k-1} \quad (38)$$

Prediction terms

$$\hat{\mathbf{x}}_{k+1|k} = \mathbf{F}(\hat{\mathbf{x}}_{k|k}, \mathbf{u}_k) \quad (39)$$

$$\mathbf{P}_{k+1|k} = \mathbf{A}_{k|k} \mathbf{P}_{k|k} \mathbf{A}_{k|k}^T + \mathbf{Q} \quad (40)$$

with

$$\mathbf{A}_{k|k} = \left. \frac{\partial \mathbf{F}}{\partial \mathbf{x}} \right|_{\mathbf{x}_{k|k}} \quad (41)$$

$$\mathbf{H}_{k|k-1} = \left. \frac{\partial \mathbf{h}}{\partial \mathbf{x}} \right|_{\mathbf{x}_{k|k-1}} \quad (42)$$

Here, $\mathbf{x}_{k|j}$ denotes the estimated state vector at time t_k based on the measurements up to time t_j . Model eqs 32 can be either the model with CSTR jacket or the model with a tubular jacket. For calorimetry performed by a state estimator, the heat of reaction Q_R and the heat-transfer coefficient k are treated as pseudo-parameters with constant values. The nonlinear estimation system is then extended to

$$\begin{aligned}\dot{\mathbf{z}} = \begin{pmatrix} \dot{\mathbf{x}} \\ \dot{\mathbf{p}} \end{pmatrix} &= f \begin{pmatrix} x, p, u \\ 0 \end{pmatrix} + \xi(t) \\ \mathbf{z}(0) &= \mathbf{x}_0 \quad \mathbf{p}_0 + \xi_0\end{aligned}\quad (43)$$

$$\mathbf{y}(t) = \mathbf{h}(x) + \varphi(t) \quad (44)$$

4.2. Calorimetry Using the EKF. The liquid level in the vessel is assumed to be known either from measurements or from open-loop simulation and can therefore be considered as an input to the state estimator model. Thus, the heat capacity (C_S) is changed only by the volume increase and by the change of the composition of the reactor contents. Average values $c_{p,R}$ and $c_{p,R,in}$, are calculated and considered to be constant for one time step. As the composition in the tank will not change as rapidly as the temperatures, this is a plausible assumption.

For the sake of clarity, we have assumed that C_{equip} is negligible and that $\rho_R c_{p,R} = \rho_{RC} c_{p,R}$. If the heat capacities of the different components in the reactor and the feed are very different, this simplification cannot be made. Also, we combine $\dot{Q}_{R,source} + \dot{Q}_{R,loss}$ into \dot{Q}_R (as they are not observable separately).

A partial differential equation cannot be used directly in the EKF. Some form of discretization is necessary. The tubular behavior of the jacket can be approximated well using orthogonal collocation.^{19,20} To yield an acceptable model, it is sufficient to use four to six internal collocation points, resulting in five to seven differential equations for the lower part of the jacket instead of one. Such a discretized model provides good accuracy. It has also been shown that orthogonal collocation preserves observability.²¹ Therefore, this method is a suitable approach for the problem at hand. The application of orthogonal collocation yields

$$\frac{d}{dt} X(t) = -\frac{m_J}{bhL\rho_J} \mathbf{B}X(t) - \frac{m_J}{bhL\rho_J} \mathbf{B}_{z=0} x(t, z=0) + \frac{k}{\rho_J c_{p,J} b} F(X(t)) \quad (45)$$

with

$$X(t) = \begin{pmatrix} T_{J,L}(z=z_1) \\ T_{J,L}(z=z_2) \\ \vdots \\ T_{J,L}(z=z_{p+1}) \end{pmatrix} \quad (46)$$

$$F(X(t)) = \begin{pmatrix} T_R - T_{J,L}(z=z_1) \\ T_R - T_{J,L}(z=z_2) \\ \vdots \\ T_R - T_{J,L}(z=z_{p+1}) \end{pmatrix} \quad (47)$$

The boundary condition $x(t, z=0) = T_{J,in}$ is an input variable to the above system of ordinary differential equations.

Table 1. Physical Constants and Their Values Used in the Simulation Studies

label	value	units	label	value	units	label	value	units
b	0.01	m	$[I]^w(t=0)$	4.48×10^{-5}	kmol/m ³	$n_M(t=0)$	0.5×10^{-2}	kmol
C_{equip}	2	kJ/K	k_0	0.7	kW/(m ² K)	$n_X(t=0)$	0.025×10^{-6}	kmol
c_{pJ}	1.2	kJ/(kg K)	k_{fX}	$21k_p$	L/(mol s)	N_T	6×10^{21}	
c_{pM}	1.5	kJ/(kg K)	k_1	4×10^{-5}	1/s	T_{in}	293	K
c_{pPol}	1.8	kJ/(kg K)	k_M^d	2700		$T_R(t=0)$	333	K
c_{pW}	4.2	kJ/(kg K)	k_M^p	1500		$V_P(t=0)$	0.35	L
c_{pX}	2	kJ/(kg K)	k_p	176	L/(mol s)	$V_W(t=0)$	5	L
D_M^P	1×10^{-10}	m ² /s	k_t	4.32×10^7	L/(mol s)	ΔH_R	-73×10^3	kJ/(mol K)
D_M^W	$\times 10^{-10}$	m ² /s	k_X^d	700		Δk	0.63	kW/(m ² K)
d_R	0.25	m	k_X^k	450		ρ_J	800	kg/m ³
f	0.6		m_J	0.1	kg/s	ρ_M	904	kg/m ³
F_p	1×10^{-3}		M_M	104.1	g/mol	ρ_{Pol}	1050	kg/m ³
h	0.04	m	M_W	18.02	g/mol	ρ_X	842	kg/m ³
$[I]^F$	1×10^{-2}	kmol/m ³	M_X	90.2	g/mol			

p is the number of internal collocation points, and z describes the space domain. \mathbf{B} and $\mathbf{B}_{z=0}$ are the collocation matrices. Therefore, z_{p+1} corresponds to the effective length of the jacket pipe, up to where exchanging heat is possible. L appears in the denominator of the factors, as orthogonal collocation is always normalized onto the interval.^{0,1} The expression for \hat{Q}_J

$$\hat{Q}_J(t) = \int_0^L kh[T_R(t) - T_{J,L}(z, t)] dz \quad (48)$$

is integrated using the trapezoid rule along the collocation points.

The model describing the upper part of the jacket is solved for one collocation point. Discretizing the equation for the upper part of the jacket results in the subsequent expression

$$\frac{dT_{J,U}}{dt} = -\frac{\dot{m}_J}{bh\rho_J(L_{\text{max}} - L)}[T_{J,L}(z = z_{p+1}) + T_{J,U}(z = z_{p+1})] \quad (49)$$

The EKF model now consists of the expression

$$\frac{dT_R}{dt} = \frac{\dot{V}_{R,in}}{V_R}(T_{R,in} - T_R) + \frac{\hat{Q}_R}{V_R\rho_R c_{p,R}} - \hat{Q}_J$$

and eqs 43, 46, and 47. The model used in the observer is extended by the following two equations

$$\frac{d\hat{Q}_R}{dt} = 0 \quad (50)$$

$$\frac{dk}{dt} = 0 \quad (51)$$

to estimate \hat{Q}_R and k .

It has to be noted that the models derived above are globally observable if $T_J \neq T_R$. If the two temperatures are equal, then k cannot be estimated as no heat is transferred, i.e., the system is unobservable.

4.3. EKF Tuning. As discussed in refs 17 and 20, the weighting matrix \mathbf{Q} of the EKF has to be adjusted to changes in the dynamic behavior of the process. By investigation of the eigenvalues of the reactor model, it was found that the most important change of the dynamics is caused by the mass flow rate of the coolant and that the estimation of the heat of reaction is most sensitive to this change. Thus, the diagonal element $q_{\hat{Q}_R}$ of the tuning matrix \mathbf{Q} of the EKF was adapted

by a factor $\dot{m}_J/\dot{m}_{J,\text{min}}$ that compensates for the eigenvalue change by increasing the amplification. In this way, \hat{Q}_R is corrected more strongly, and this facilitates the estimation of k . The physical interpretation of this change is as follows: An increase in the jacket mass flow rate reduces the resulting ΔT , which is directly used in the state estimation scheme and directly reflects \hat{Q}_R . This adaptation improves the estimation result considerably. The resulting EKF yields good estimation results for a range of different flow rates.

4.4. Open-Loop Estimation of the Missing States.

The estimated value of \hat{Q}_R can be used in the provided simulation model to estimate the remaining parameters that are required in the control scheme. The method is used similarly in ref 1. Assuming that \hat{Q}_R is now known, the following simplified simulation model can be derived, which is run in parallel to the process. Using eq 22, the following mass balance equations result

Molar balance of monomer

$$\frac{dn_M}{dt} = \frac{d}{dt}([M]V_R) = \dot{n}_M - \frac{\hat{Q}_R}{-\Delta H} \quad (52)$$

Molar balance of CTA

$$\frac{dn_X}{dt} = \frac{d}{dt}([X]V_R) = \dot{n}_X - \frac{k_{fX}[X]^p}{k_p[M]^p} \frac{\hat{Q}_R}{-\Delta H} \quad (53)$$

Equations 63–73 are then no longer required. Their purpose is only to calculate \bar{n} , which is now determined by calorimetry. The phase distribution and the molecular weight distribution can be calculated as detailed in Appendices A and C.

It should be noted that this open-loop estimation will yield persistent errors if either \hat{Q}_R or the initial conditions are not estimated well.²²

5. Simulation Studies

The hierarchical control approach presented here is applied to the seeded semibatch emulsion polymerization of styrene with butyl maleate (BuM). BuM acts as a chain-transfer agent. The process is operated at 60 °C. Both styrene and BuM are fed continuously to the reactor. Hence, the manipulated variables are the feed rates of monomer and CTA and the jacket inlet temperature. The rigorous model is used to simulate the process in a 10l stainless steel reactor. Geometric,

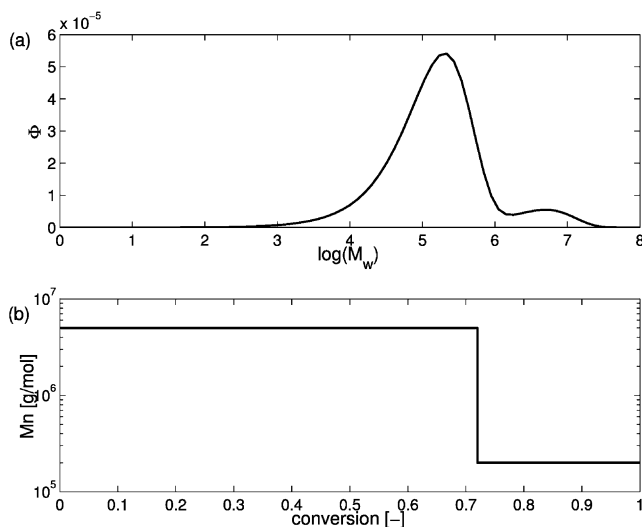


Figure 4. (a) Desired bimodal MWD and (b) set points of the average molecular weight.

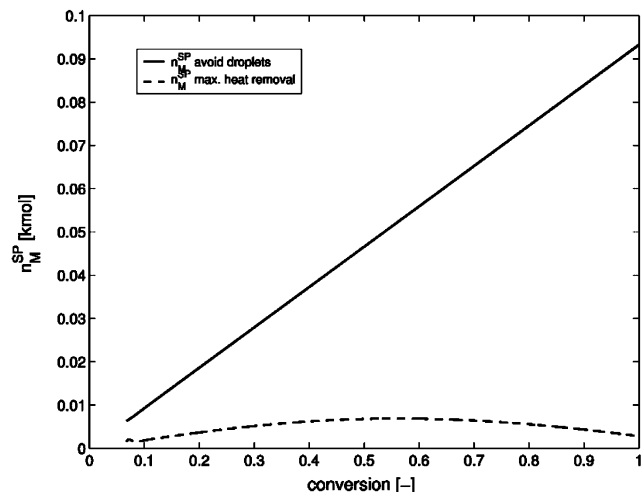


Figure 5. Constraints of the molar monomer holdup in the reactor calculated by step 3 of the control approach.

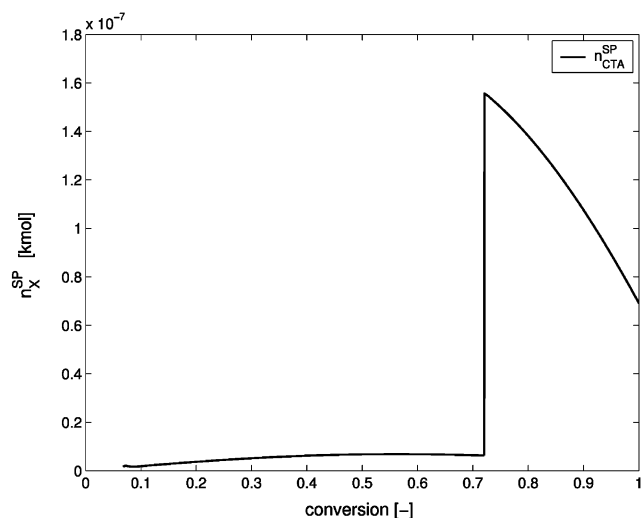


Figure 6. Set point of the molar CTA holdup in the reactor calculated by step 5 of the control approach.

physical, and process operating data were obtained from a pilot plant at the Process Control Laboratory at the Universität Dortmund. The reactor is sketched in Figure 1. The jacket is constructed as a spiral channel.

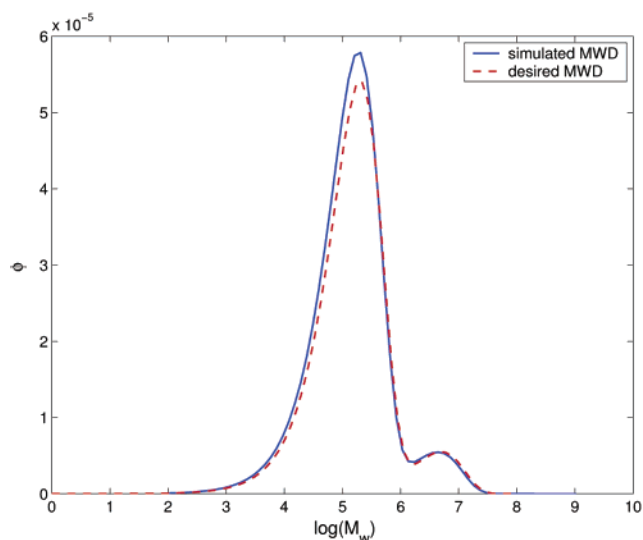


Figure 7. Comparison of the desired and produced MWDs.

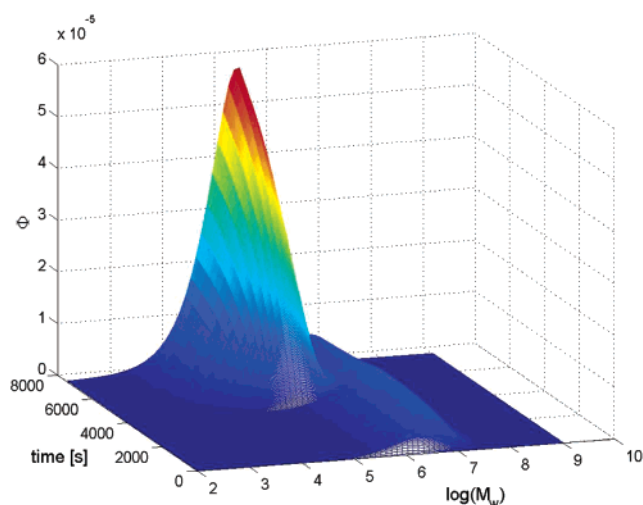


Figure 8. Development of the MWD over process time.

We assume that the heat-transfer coefficient decreases with increasing conversion, i.e., with increasing solids content, modeled by

$$k = k_0[1 - (\Delta k)X_C^{2/3}] \quad (54)$$

where X_C denotes the conversion of the monomer, k_0 is the heat-transfer coefficient for the reactor charged with water, and Δk is an adjustable parameter.

The physical constants used in the simulations are taken from ref 1, where it was shown that the model represents reality well. They are also provided in Table 1.

An example of a desired bimodal molecular weight distribution is displayed in Figure 4a. The set points of the average molecular weight are calculated off-line by the method given in section 3.1. It is advisable that the polymer with the largest molecular weight be produced first.¹ If, instead of BuM, a slow-reacting CTA is used, e.g., CCl_4 , its accumulation in the reactor will prevent the production of long-chain polymers at the end of the batch.

The ratio of the concentrations of monomer and CTA in the particle phase is found from the optimization as described in section 3.1. The result of the calculations performed in step 3 of the hierarchical control approach

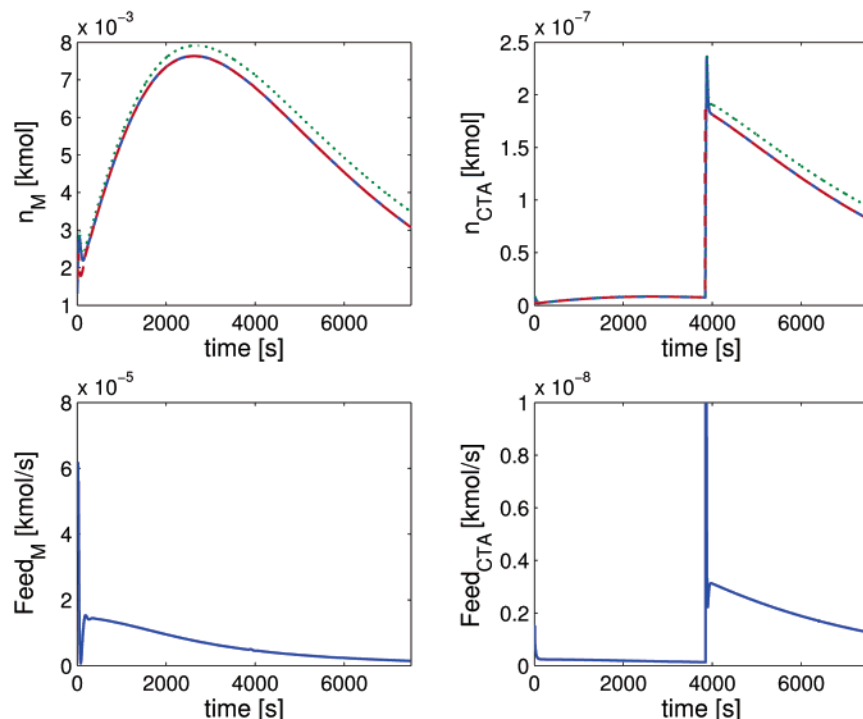


Figure 9. Results of the proposed control approach: (···) molar holdup in the simulation of the rigorous model, (---) set point calculated by the proposed hierarchical control scheme, (—) estimation of the holdup and the calculated feed rates.

is depicted in Figure 5. It can be seen clearly that the process operation is restricted by the heat removal capacity, i.e., the polymer seed is able to absorb more monomer than allowed in the reactor for a thermally safe process operation. Note that the curves will change with the geometry of the reactor and its heat-transfer properties. In laboratory-scale reactors, for example, the avoidance of a droplet phase will be limiting at the beginning of the process because of the favorable ratio between the heat-transfer area and the reactor volume and the comparably high jacket flow rate. For such small reactors, the limiting condition will switch during the process as the ability to store monomer in the particle phase will increase with the solids content whereas the heat transfer will decrease.

From the calculated set point of the molar holdup of styrene in the reactor, the amount of CTA is determined by step 5 of the control approach (Figure 6). Obviously, the CTA set point is determined by the desired average molecular weight (cf. Figure 4).

For these calculations, the estimated values of the heat of reaction and the heat-transfer coefficient are needed. Because the jacket of the reactor considered here is described by a tubular model, we apply the EKF with the tubular model.

The control approach is tested with respect to the true goal, namely, the production of a desired MWD. Figure 7 shows that the desired final bimodal MWD is produced sufficiently accurately. This results from the good performance of the decentralized PI controllers. The development of the MWD over the batch is shown in Figure 8. The set-point change can be seen clearly. Figure 9 depicts the set-point tracking for the monomer and the CTA holdup in the reactor for the PI controllers used here.

Figure 9 shows that the molar holdups simulated by the open-loop observer deviate from the true values. The

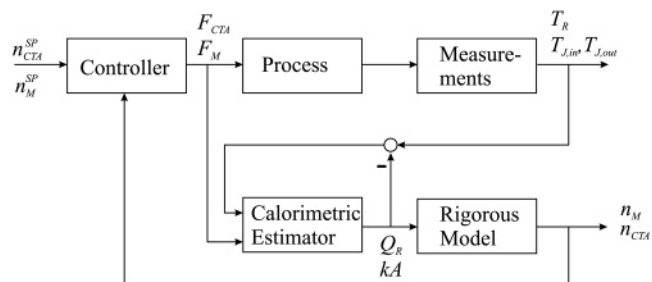


Figure 10. Control scheme.

controller receives the estimates of these true values and controls them to match the set point exactly. The offset between the estimates and the true values is caused by the applied control scheme using an open-loop observer (see Figure 10). Even if the initial load of monomer and CTA is known, the initial guess for the heat of reaction is usually not equal to the true value. The consumption of monomer by the reaction is calculated in the open-loop observer using the estimated heat of reaction. Hence, the initial convergence of the calorimetric estimator yields a monomer consumption rate that is different from the true one and consequently causes different initial conditions for the molar holdups of the open-loop observer. Additionally, it has to be considered that the produced heat of reaction is a transient process. In contrast, the assumption behind the parameter estimation scheme is a stepwise-constant disturbance. Typically, the disturbance estimation is not able to track the true disturbances exactly (compared to a PI controller that is not able to track a ramp of the set point exactly) and causes the same behavior of the open-loop observer as described in Figure 9.

For the control problem at hand, the difference is not important, as the reaction rates of both reactants are determined by the estimated heat of reaction and are

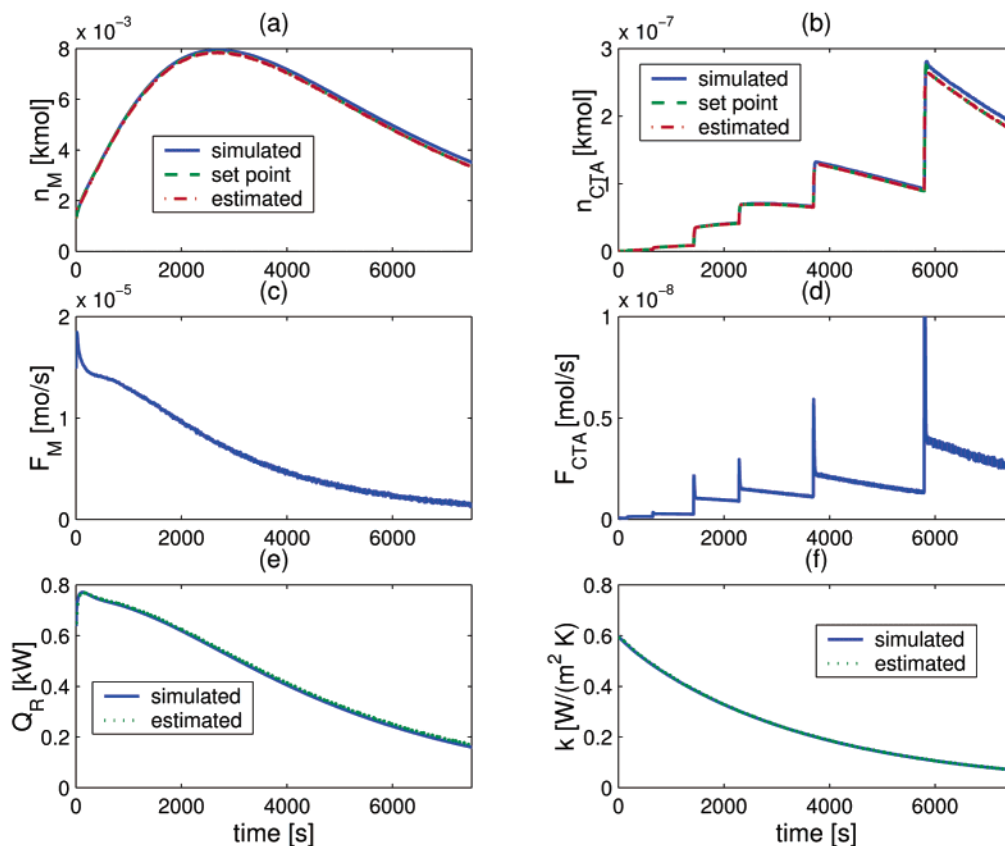


Figure 11. Simulated process to produce a polymer with a broad MWD: (a) molar holdup of monomer, (b) molar holdup of CTA, (c) feed monomer, (d) feed CTA, (e) heat of reaction, (f) heat-transfer coefficient.

not based on the estimated absolute values of the holdups of monomer and CTA

$$r_M^p = k_p [M]^p \frac{\bar{n} N_p}{N_T} = \frac{\dot{Q}_R}{-\Delta H} \quad (55)$$

$$r_X^p = k_{f,X} [X]^p \frac{\bar{n} N_p}{N_T} = \frac{\dot{Q}_R}{-\Delta H} \frac{k_{f,X} [X]^p}{k_p [M]^p} \quad (56)$$

Hence, the trajectory of the ratio between the monomer and CTA holdups, and therefore the average molecular weight, is tracked well.

To demonstrate the performance of the proposed control scheme, in a second experiment, the production of a broad unimodal MWD is considered, i.e., for a polydispersity index of the final distribution $PDI > 2$. A unimodal MWD with large polydispersity can be produced by changing the ratio between monomer and CTA, with this conversion being made in a stepwise or linear fashion. In the simulation study, we consider a stepwise change of the desired average molecular weight to show the set-point tracking of the decentralized linear PI controllers. Figure 11 shows the results for a simulated semibatch emulsion polymerization of styrene with butyl maleate as the CTA. The measurements of the different temperatures were disturbed by measurement noise and are available at a sample time of 2 s. Subfigures e and f demonstrate the performance of the applied EKF. The heat of reaction as well as the heat-transfer coefficient are estimated very well. Based on this information, the calculated molar holdups are close to the true values (see subfigures a and b). Once again, it can be observed that the open-loop observer is not able to compensate for the inaccurate initial conditions. The

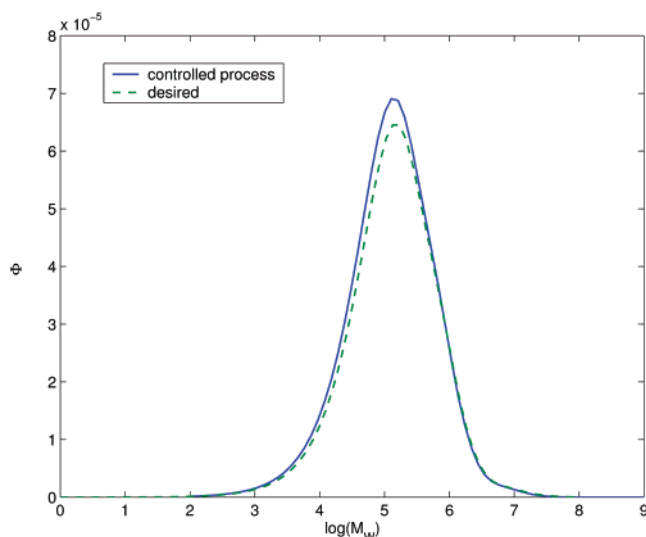


Figure 12. Desired and achieved MWDs for a unimodal broad distribution.

set-point curve of the monomer results from the constraint of the limited heat removal capacity of the reactor, whereas the trajectory of the CTA is determined from the desired average molecular weight, i.e., from the necessary ratio between the concentrations of monomer and CTA in the polymer particle phase. Both are tracked well by the decentralized time-discrete PI controllers. Subfigures c and d depict the behavior of the manipulated variables. No restrictions on the dynamic behavior of the manipulated variables have been considered, which enables the design of fast controllers. The peaks are overshoots that appear as impulses because of the scaling of the x axis.

Figure 12 compares the achieved MWD and the desired MWD. It can be stated that the goal is achieved sufficiently well. Hence, by the proposed control approach, it is possible to produce arbitrary molecular weight distributions for processes with a CTA-dominated termination reaction in minimal time.

6. Conclusions

A hierarchical approach to the time-optimal operation of a semibatch emulsion polymerization using a new technique to calculate the set points of the molar holdups of the reactants was derived. The approach uses a state estimator [extended Kalman filter (EKF)] to estimate the heat of reaction and the heat-transfer coefficient for the jacket cooling. The advantage of the proposed control scheme is three-fold: (1) Numerical optimization to calculate a time-optimal trajectory is avoided. All necessary calculations are algebraic in nature and can easily be performed on-line. (2) Linear decentralized controllers can be applied. This is of special interest in industrial-scale applications. (3) The approach is able to handle drifts in the heat-transfer properties and to reject disturbances of process conditions.

We focused on the control of pilot-scale and industrial-size reactors. Medium-size reactors especially pose considerable problems. Special attention has to be paid to the fact that reactors of larger volumes use a jacket that behaves not like an ideal continuously stirred tank reactor (CSTR) but more like a plug-flow reactor (PFR). The novelty of the proposed hierarchical control scheme is based on identifying limiting constraints of the process at which a maximum propagation reaction rate is achieved. These boundaries are the avoidance of the formation of a droplet phase and the limiting heat removal capacity, which is very important for larger reactors. To drive the process at its maximum heat removal capacity, a reliable estimation of the heat-transfer coefficient is needed. A poor estimate of this parameter might lead to dangerous process operation if the heat removal capacity is overestimated. Thus, an accurate model of the jacket is needed. It has also been shown that, for a homopolymerization using a CTA, decentralized linear controllers are sufficient to achieve a good control performance.

The extension of the proposed approach to control the copolymer composition is currently being investigated.

Acknowledgment

Parts of this work were funded by the DFG (Deutsche-Forschungs-Gemeinschaft), DFG-Project EN 152/31-1. The authors gratefully acknowledge this financial support.

Appendix A. Emulsion Homopolymerization Model Equations

A.1. Model Equations. This appendix provides the model equations used for process simulation. The symbols can be found in the Nomenclature section. If equations are taken from the literature, the source is indicated.

First, molar balances of the monomer and chain-transfer agent (CTA) chain-transfer agent are set up as follows:

Molar balances of monomer and CTA

$$\frac{dn_M}{dt} = \dot{n}_M - V^p r_M^p \quad (57)$$

$$\frac{dn_X}{dt} = \dot{n}_X - V^p r_X^p \quad (58)$$

where n_M is the number of moles of monomer in the system (i.e., in all phases combined); n_X is the number of moles of CTA in the system; V^p is the volume of the particulate phase; r_M^p is the monomer reaction rate in the particulate phase; r_X^p is the CTA reaction rate in the particulate phase; and \dot{n}_M and \dot{n}_X are the molar feed rates of monomer and CTA, respectively. If water is added in the form of pure water or initiator or emulsifier solution, a water balance is necessary.

Water balance

$$\frac{dV_W}{dt} = \dot{V}_W + \dot{V}_I + \dot{V}_E = \bar{V}^w \quad (59)$$

where V_W is the volume of water in the system and \dot{V}_W , \dot{V}_I , and \dot{V}_E are the addition rates of water, initiator solution, and emulsifier solution, respectively. The molar balance of initiator reads

Initiator balance

$$\frac{dn_I}{dt} = \dot{V}_I [I]^F - f k_I [I]^w V^w \quad (60)$$

where n_I is the number of moles of initiator, $[I]^F$ the initiator feed concentration, f is the decomposition rate efficiency factor to account for the cage effect, and k_I is the initiator decomposition rate constant. $[I]^w$ is the initiator concentration in the water phase, and V^w is the volume of the water phase. A polymer volume balance is also calculated.

Polymer volume balance

$$\frac{dV_{Pol}^p}{dt} = V^p r_M^p \frac{M_M}{\rho_{pol}} \quad (61)$$

where V_{Pol}^p is the volume of polymer in the polymer phase, M_M is the molecular weight of the monomer, and ρ_{pol} is the density of the polymer. The following reaction rates are necessary for the above equations

Reaction rates

$$r_M^p = k_p [M]^p \frac{\bar{n} N_T}{N_A V^p} \quad (62)$$

$$r_X^p = k_{tX} [X]^p \frac{\bar{n} N_T}{N_A V^p} \quad (63)$$

where k_p and k_{tX} are the propagation and chain-transfer rate coefficients, respectively; \bar{n} is the average number of radicals per particle; and N_T is the number of particles. Thus, $\bar{n} N_T / N_A V^p$ denotes the concentration of radicals in the particle phase.

Emulsion polymerization is a three-phase process. The phase distribution is calculated using constant partition coefficients^{23,24} and an algorithmic solution (see Appendix B). V_i^w is the water-phase volume of

monomer (V_M^w) or CTA (V_X^w). V_i is the total volume of species i in the system, and \underline{V}_i is its molar volume. After all volumes are known, the needed individual concentrations can be calculated as

$$[i]^j = \frac{V_i^j}{\underline{V}_i V^j} = \frac{n_i^j}{V^j} \quad (64)$$

The two important quantities in the reaction rates are the average number of radicals per particle (\bar{n}) and the number of particles. In this model, it is assumed that the number of particles is known and constant. Therefore, only a model of \bar{n} is needed. A concise differential equation for the average number of radicals in the particle phase is used here.

Average number of radicals per particle²⁵

$$\frac{d\bar{n}}{dt} = k_a [R]^w - k_d \bar{n} - \varphi_N c \bar{n}^2 \quad (65)$$

with

$$\varphi_N = \frac{2(2k_a [R]^w + k_d)}{2k_a [R]^w + k_d + c} \quad (66)$$

$$c = \frac{k_T^p N_T}{N_A V^p} \quad (67)$$

where φ is an approximate solution of the first moment of the distribution N_i and N_i is the number of particles with i radicals. k_d and k_a are particle desorption and absorptions rate constants, respectively. $[R]^w$ is the concentration of radicals in the water phase, and k_T^p is the termination rate constant in the particle phase. A radical balance for the water phase is necessary. If the number of particles is constant, then either coagulation and nucleation effects are balanced, or they are both zero. If nucleation is considered to be zero, then population balances of the radicals in the water phase, n_R^w , are not necessary. A lumped radical balance is used.

Radical balance for the water phase²⁶

$$\frac{dn_R^w}{dt} = 2fk_I [I]^w V^w + k_d \bar{n} \frac{N_T}{N_A} - k_a [R]^w \frac{N_T}{N_A} - k_t^w ([R]^w)^2 V^w \quad (68)$$

$$[R]^w = \frac{n_R^w}{V^w} \quad (69)$$

k_T^j is the termination rate in phase j , whereby the termination in the particles phase varies because of the gel effect. The gel effect is considered using a semiempirical relationship.

Gel effect (semiempirical²⁷)

$$k_t^p = k_t^w \exp(-\alpha_1 \Phi_{Pol}^p) \quad (70)$$

where $\alpha_1 = 2$ for the simulation but, in general, is an adjustable parameter and Φ_{Pol}^p is the volume fraction of polymer in the particle phase. The absorption rate is

calculated according to the following expression

Absorption rate²⁸

$$k_a^i = 4\pi D_i^w r_p N_A F_p \quad (71)$$

$$k_a = \sum_{i \in M, X} k_a^i \quad (72)$$

where D_i^w is the diffusion coefficient of radicals in water, F_p is the absorption efficiency (adjustable), and r_p is the radius of a single particle.

Particle radius

$$r_p = \sqrt[3]{\frac{3V^p}{4N_T \pi}} \quad (73)$$

Desorption is calculated using the following equations

Radical desorption^{29,30}

$$k_{0i} = \frac{12D_i^w}{k_i^p d_p^2} \left(1 + \frac{2D_i^w}{k_i^p D_i^p} \right) \quad (74)$$

$$\beta_i = \frac{k_t^w [R]^w + k_p [M]^w}{k_t^w [R]^w + k_p [M]^w + \frac{k_a^i N_T V^w}{V^w N_A}} \quad (75)$$

$$k_d^i = (k_{fM} [M]^p + k_{fX} [X]^p) \beta_i \frac{k_{0i}}{k_{0i} \beta_i + k_p [M]^p} \quad (76)$$

$$k_d = \sum_i k_d^i \quad (77)$$

where k_{0i} is the constant of the diffusional exit rate of a radical of type i as derived in ref 31. D_i^w and D_i^p are the diffusion coefficients of radicals of type i in the water and the particle phases, respectively. k_i^p is the partition coefficient of monomer between water and the particle phase. As an approximation, this parameter is also used to describe the partitioning of radicals between these two phases. d_p is the diameter of a particle. β_i defines the probability that a monomer or CTA radical reacts in the water phase. i always represents M or X. In this approach, the CTA radical is considered to be as reactive as the monomer or initiator radical.

Further equations are required for the calculation of the molecular weight distribution:

Instantaneous number-average chain length³²

$$\bar{M}_n = \frac{r_p^p}{r_T^p} \quad (78)$$

where r_T^p is the termination rate

Termination rate: general

$$r_T^p = (k_{fX} [X]^p + k_{fM} [M]^p + k_a [R]^w) \frac{\bar{n} N_T}{N_A V^p} \quad (79)$$

If CTA is considered the main termination event, this equation can be simplified as follows

Termination rate: CTA main termination event

$$r_T^p = k_{TX}[X]^p \frac{\bar{n}N_T}{N_A V^p} \quad (80)$$

The distribution calculation is performed using the derivation in Appendix C.

Instantaneous normalized molecular weight distribution (see Appendix C)

$$W(n) = \frac{n}{\bar{M}_n^2} \exp\left(-\frac{n}{\bar{M}_n}\right) \quad (81)$$

Molecular weight distribution (see Appendix C)

$$\frac{d}{dt}W_T(n) = \frac{dX_C}{dt} \frac{1}{X_C} [W(n) - W_T(n)] \quad (82)$$

The calculation is based on the total conversion

Total conversion X_C

$$\frac{dX_C}{dt} = \frac{\dot{n}_M + n_X - \frac{dn_M}{dt} - \frac{dn_X}{dt}}{n_M^T + n_X^T} \quad (83)$$

where n_M^T and n_X^T denote the total amounts of monomer and CTA, respectively, fed to the reactor.

Appendix B. Phase Distribution Calculation

The phase distribution calculation is taken from Arzamendi et al.²⁴ For large diffusion rates, i.e., instantaneous mass transfer, the partition coefficients are given as

$$k_i^d = \frac{V_i^d/V^d}{V_i^w/V^w} \quad (84)$$

$$k_i^p = \frac{V_i^p/V^p}{V_i^w/V^w} \forall i \quad (85)$$

where V^d is the total droplet phase volume and V_i^d is the droplet-phase volume of monomer i . $2i$ equations result. If the relevant balance equations are written, a further $3 + i$ equations result

$$V^d = \sum_{i=1}^n V_i^d \quad (86)$$

$$V^p = V_{Pol} + \sum_{i=1}^n V_i^p \quad (87)$$

$$V^w = V_W + \sum_{i=1}^n V_i^w + V_I + V_R \quad (88)$$

$$V_i = V_i^w + V_i^d + V_i^p \quad (89)$$

An equation system with $3 + 3i$ equations, $2i$ constants (partition coefficients), and $5 + 4i$ variables

results. V_{Pol} , V_W , and V_i are states of the model, resulting in a remaining $3 + 3i$ unknowns.

If the droplet phase disappears, k_i^d in eq 80 is undefined; eqs 80 and 82 disappear; and the variables k_i^d , V_i^d , and V^d have to be eliminated from all equations. A new and incompatible equation system results. As such, this solution is problematic in a standard solver. Therefore, the solver needs to identify, when the droplet phase disappears and then switch between the equation systems.

To avoid the need to solve a switched differential algebraic equation (DAE), an algorithmic solution to the problem that can handle the existence and absence of the droplet equally well is used.³³

Using the volumes V_i , V_{Pol} , and V_W provided by the dynamic model as well as the partition coefficients k_i^d and k_i^p , the iterative algorithmic solution proceeds as follows:

From eqs 84 and 85

$$V_i^d = \frac{V^d}{V^p} \frac{k_i^d}{k_M^p} V_i^p \quad (90)$$

Equation 85 yields

$$V_i^w = \frac{V^w}{V^p} \frac{1}{k_i^p} V_i^p \quad (91)$$

Equations 89–91 can now be combined to give

$$V_i^p = \frac{V_i}{1 + \frac{V^w}{V^p k_i^p} + \frac{V^d k_i^d}{V^p k_i^p}} \quad (92)$$

These equations are used in the following algorithm:

1. The initial conditions for V^d , V^p , and V^w are guessed.

2. The volumes

$$V_i^p = \frac{V_i}{1 + \frac{V^w}{V^p k_i^p} + \frac{V^d k_i^d}{V^p k_i^p}} \quad (92)$$

are calculated using V_i provided by the differential equations.

3. The volumes

$$V_i^w = \frac{V^w}{V^p} \frac{1}{k_i^p} V_i^p \quad (91)$$

and

$$V_i^d = \frac{V^d}{V^p} \frac{k_i^d}{k_M^p} V_i^p \quad (90)$$

are calculated.

4. The new values for V^d , V^p , and V^w are calculated from eqs 86–88.

5. The iteration is continued until convergence is reached.

6. The concentrations in the phases, if needed, can be calculated as

$$[M^i]^p = \frac{V_i^p}{V^p M_i} \quad (93)$$

This algorithm shows rapid, stable convergence for reasonable initial conditions and handles the existence and absence of monomer droplets equally well.

Appendix C. Molecular Weight Calculation

The molecular weight calculation is on the basis of the idea that the final molecular weight distribution can be expressed as the integral over the instantaneous molecular weight distributions during the process operation. This concept has been proposed by a number of authors.^{1,6,34} They have shown that it is valid if the transfer reactions are dominated by the CTA. When 0–1 kinetics are assumed, the instantaneous number-average chain length (\bar{M}_n) can be expressed as the ratio between propagation and termination, as the length of a chain depends on the number of propagation steps between one termination step³²

$$M_n = \frac{r_M^p}{r_T^p} \quad (94)$$

The termination rate is given by the chain-transfer and absorption rates, as for 0–1 kinetics, an absorbed radical either grows or terminates instantaneously

$$r_T^p = (k_{IX}[X]^p + k_{IM}[M]^p + k_a[R]^w) \frac{\bar{n}N_T}{N_A V^p} \quad (95)$$

If the transfer to CTA is the main termination event, eq 95 can be simplified to

$$r_T^p = k_{IX}[X]^p \frac{\bar{n}N_T}{N_A V^p} \quad (96)$$

An instantaneous normalized molecular weight distribution [$\bar{W}(n)$] of the form

$$\bar{W}(n) = \frac{n}{\bar{M}_n^2} \exp\left(-\frac{n}{\bar{M}_n}\right) \quad (97)$$

is used. The full derivation can be found in refs 1 and 34. It is redeveloped here for clarity:

Let \bar{M}_n be the instantaneous number-average chain length, which is assumed to be known. According to ref 35 (p 64), the Schulz–Zimm distribution is the correct distribution for instantaneous chain length distribution calculation.

It can be found in ref 9 (p 68) that, for “low conversion and polymer made to have a certain molecular weight” and termination by disproportionation or chain transfer, the polydispersity index is 2. These conditions are fulfilled for the instantaneous molecular weight distribution.

The instantaneous chain length distribution as a Schulz–Zimm distribution is given by

$$\bar{M}(n) = \frac{\left(\frac{l}{\bar{M}_n}\right)^{(l+1)} n^{l-1} \bar{M}_n \exp\left(-l\frac{n}{\bar{M}_n}\right)}{\Gamma(k+1)} \quad (98)$$

$$l = \frac{\bar{M}_n}{\bar{M}_w - \bar{M}_n} \quad (99)$$

where Γ is the gamma function, l is the coupling number, and n is the chain length currently being considered. The coupling l is normally 1 for instantaneous termination by disproportionation. Using $l = 1$ thus leads back to a polydispersity index of 2, if used in eq 99.

Using either the polydispersity index of 2 or $l = 1$ and the definition of the polydispersity index as the ratio between the instantaneous number-average chain length (\bar{M}_n) and the instantaneous weight-average molecular weight (\bar{M}_w), the following equation can be written

$$2 = \frac{\bar{M}_w}{\bar{M}_n} \quad (100)$$

Inserting eq 100 into eq 99 or simply setting $k = 1$ simplifies the Schulz–Zimm distribution in eq 98 to

$$\bar{M}(n) = \frac{1}{\bar{M}_n} \exp\left(-\frac{n}{\bar{M}_n}\right) \quad (101)$$

Note that the Schulz–Zimm distribution always calculates the normalized number average. However, in this case, a normalized molecular weight distribution is required. To achieve this, the definition of the normalized distribution functions are used. They can be written as

$$\bar{M}(n) = \frac{M(n)}{\sum_{i=1}^{\infty} M(i)} \quad (102)$$

$$\bar{W}(n) = \frac{W(n)}{\sum_{i=1}^{\infty} W(i)} \quad (103)$$

where $M(n)$ provides the number of chains in the population with chain length n and $\bar{M}(n)$ is the probability that a chain that is randomly picked from the population is of length n . $\bar{W}(n)$ provides the total weight of chains in the population with chain length n , and $\bar{W}(n)$ is the weight fraction of all chains of length n . $W(n)$ is the molecular weight distribution.

The two distributions $M(n)$ and $W(n)$ are linked by the following equation

$$W(n) = M(n)nM_M \quad (104)$$

where M_M is the molecular weight of the monomer. From this relationship, the relationship between the

normalized distributions can be derived as

$$\begin{aligned}
 W(n) &= M(n)nM_M \\
 \bar{W}(n) &= \frac{W(n)}{\sum_{i=1}^{\infty} W(i)} = \frac{M(n)nM_M}{\sum_{i=1}^{\infty} W(i)} \\
 \bar{W}(n) &= \frac{M(n)nM_M}{\sum_{i=1}^{\infty} M(i)iM_M} \\
 &= \frac{M(n)n}{\sum_{i=1}^{\infty} M(i)i} \\
 &= n \frac{M(n)}{\sum_{i=1}^{\infty} M(i)} \left[\frac{\sum_{i=1}^{\infty} M(i)i}{\sum_{i=1}^{\infty} M(i)} \right]^{-1} \\
 &= \frac{n\bar{M}(n)}{\bar{M}_n} \quad (105)
 \end{aligned}$$

The result in eq 105 can now be used in eq 101 to yield the normalized molecular weight distribution

$$\bar{W}(n) = \frac{n}{\bar{M}_n^2} \exp\left(-\frac{n}{\bar{M}_n}\right) \quad (106)$$

The total normalized molecular weight distribution at time t [$\bar{W}_T(n)$] is thus the integral over the batch up to the current conversion X_C

$$\bar{W}_T(n) = \frac{1}{X_C} \int_0^{X_C} \bar{W}(n) dX \quad (107)$$

It should be noted that the integration is possible because normalized distributions are considered. By differentiating eq 107 with respect to t , the following differential equation can be obtained

$$\frac{d}{dt} \bar{W}_T(n) = \frac{dX_C}{dt} \frac{1}{X_C} [\bar{W}(n) - \bar{W}_T(n)] \quad (108)$$

The total conversion X_C has to be defined for the total formulation, i.e.

$$\begin{aligned}
 X_C &= \frac{n_M(t=0) + \int_0^t \dot{n}_M d\tau + n_X(t=0)}{n_M^T + n_X^T} + \\
 &\quad \frac{\int_0^t \dot{n}_X d\tau - n_M(t) - n_X(t)}{n_M^T + n_X^T} \quad (109)
 \end{aligned}$$

$$\Rightarrow \frac{dX_C}{dt} = \frac{\dot{n}_M + \dot{n}_X - \frac{dn_M}{dt} - \frac{dn_X}{dt}}{n_M^T + n_X^T} \quad (110)$$

where n_M^T and n_X^T denote the total amounts of monomer and CTA, respectively, to be fed.

Nomenclature

A = heat-transfer area
 a_1 = gel effect constant
 A_{\max} = maximum heat-transfer area covered by the jacket
 \mathbf{B} = collocation matrix
 $\mathbf{B}_{z=0}$ = collocation matrix at $z = 0$
 b = channel width
 c = molecular termination rate constant
 C_{equip} = heat capacity of the equipment
 c_{p_i} = heat capacity of species i
 c_{p_j} = heat capacity of cooling or heating medium
 CTA = chain-transfer agent
 D_i^p = diffusion coefficient of radicals of type i in the particle phase
 D_i^w = diffusion coefficient of radicals in water
 d_p = diameter of a single particle
 d_R = diameter of the tank
 dz = differential length element
 f = initiator decomposition rate efficiency factor
 $f_{M,X}$ = ratio between the concentrations of monomer and CTA in the particle phase
 F_p = absorption efficiency (adjustable)
 h = channel height
 h_R = height of liquid in the tank
 $h_{R,\max}$ = maximum liquid level in the tank
 $[i]^j$ = concentration of species i in phase j
 $[I]^F$ = initiator feed concentration
 $[I]^w$ = initiator concentration in the water phase
 k = heat-transfer coefficient
 k_0 = heat-transfer coefficient in the reactor filled with water
 k_{oi} = constant of the diffusional exit rate of a radical of type i
 k_a = particle absorption rate constant
 k_d = particle desorption rate constant
 k_{tX} = chain-transfer rate coefficient
 k_i^d = partition coefficient for species i between the droplet and the water phase
 k_i^p = partition coefficient for species i between the particle and the water phase
 k_I = initiator decomposition rate constant
 k_p = propagation rate coefficient
 k_t^p = termination rate constant in the particle phase
 k_t^w = termination rate in the water phase
 L = length up to which the jacket is filled
 L_{\max} = maximum length up to which the jacket is filled
 $M(n)$ = chain length distribution function, number of chains of length n
 $\bar{M}(n)$ = normalized chain length distribution function, fraction of chains of length n
 M_i = molecular weight of species i
 m_J = mass of heating medium in the jacket
 \dot{m}_J = jacket flow rate of the cooling or heating medium
 M_M = molecular weight of the monomer
 \bar{M}_n = instantaneous number-average chain length
 \bar{M}_n = instantaneous normalized number-average chain length
 \bar{M}_w = instantaneous weight-average molecular weight
 \bar{M}_w = instantaneous normalized weight-average molecular weight
 n = length of a polymer chain
 \bar{n} = average number of radicals per particle
 N_A = Avogadro's number
 n_I = number of moles of initiator
 N_i = number of particles with i radicals
 n_M = number of moles of monomer in the system

\dot{n}_M = molar feed rate of monomer
 n_M^{SP} = set point of the number of moles of monomer in the system
 n_M^T = total amount of monomer to be fed
 n_{R_w} = number of moles of radicals in the water phase
 N_T = total number of particles
 n_X = number of moles of CTA in the system
 \dot{n}_X = molar feed rate of CTA
 n_X^{SP} = set point of the number of moles of CTA in the system
 n_X^T = total amount of CTA to be fed
 \mathbf{p} = parameter vector
 p = number of internal collocation points
 \mathbf{Q} = covariance matrix of the state of disturbances
 \dot{Q}_J = heat transferred from reactor to jacket
 \dot{Q}_R = heat of reaction
 r_M^p = reaction rate of monomer in the particle phase
 r_p = radius of a single particle
 r_T^p = total termination rate
 r^p = reaction rate of CTA in the particle phase
 \mathbf{R} = covariance matrix of the measurement disturbances
 $[\mathbf{R}]^w$ = concentration of radicals in the water phase
 T_J = jacket temperature
 $T_{J,in,min}$ = minimum jacket inlet temperature
 $T_{J,L}(z)$ = temperature distribution with the spatial coordinate in the lower part of the jacket
 $T_{J,U}(z)$ = temperature distribution with the spatial coordinate in the upper part of the jacket
 T_{ref} = reference temperature (absolute zero)
 T_R = reactor temperature
 $T_{R,in}$ = temperature of the feed stream
 \mathbf{u} = input vector
 V^d = total droplet-phase volume
 \dot{V}_E = emulsifier solution addition rate
 V_i = total volume of species i in the system
 \bar{V}_i = molar volume of species i
 \bar{V}_i^d = droplet-phase volume of species i
 \bar{V}_i^p = particulate-phase volume of species i
 \bar{V}_i^w = water-phase volume of species i
 V_I = initiator solution addition rate
 v_J = cooling or heating fluid velocity
 V^p = volume of the particulate phase
 V_{Pol}^p = volume of polymer in the particle phase
 V^w = volume of the water phase
 \bar{V}_W = volume of water in the system
 $\dot{\bar{V}}_W$ = water addition rate
 $\dot{\bar{V}}_W$ = overall feed rate of water
 $\bar{W}(n)$ = instantaneous normalized molecular weight distribution
 $W(n)$ = instantaneous molecular weight distribution
 $\bar{W}_T(n)$ = total (accumulated) normalized molecular weight distribution
 \mathbf{x} = state vector
 X_C = current conversion of the given recipe
 \mathbf{y} = measurement vector
 z = spatial coordinate

Greek Letters

β_i = probability that a monomer or CTA radical reacts in the water phase
 $(-\Delta H)$ = heat of reaction
 Δk = factor for the decrease of the heat-transfer coefficient with conversion
 φ_N = approximate solution of the first moment of the distribution N_i
 φ = measurement disturbance vector
 Φ_{Pol}^p = volume fraction of polymer in the particle phase
 ρ_i = density of species i

ρ_{Pol} = density of the polymer
 ξ = state disturbance vector

Literature Cited

- (1) Vicente, M.; Amor, S. B.; Gugliotta, L. M.; Leiza, J. R.; Asua, J. M. Control of Molecular Weight Distribution in Emulsion Polymerization Using On-Line Reaction Calorimetry. *Ind. Eng. Chem. Res.* **2001**, *40*, 218–227.
- (2) Kravaris, C.; Wright, R. A.; Carrier, J. F. Nonlinear Controllers for Trajectory Tracing in Batch Processes. *Comput. Chem. Eng.* **1989**, *13*, 73–82.
- (3) Gentric, C.; Pla, F. Experimental Study of the Nonlinear Geometric Control of a Batch Emulsion Polymerization Reactor. *Comput. Chem. Eng.* **1997**, *21*, 1043–1048.
- (4) Gentric, C.; Pla, F.; Latifi, M. A.; Corriou, J. P. Optimization and Nonlinear Control of a Batch Emulsion Polymerization Reactor. *Chem. Eng. J.* **1999**, *75*, 31–46.
- (5) Seferlis, P.; Kiparissides, C. Optimizing Control of Molecular Weight Properties for Batch Free Radical Polymerization Reactors. In *6th IFAC Symposium on Dynamics and Control of Process Systems (DYCOPS)*; Elsevier Science: New York, 2001; pp 251–256.
- (6) Clarke-Pringle, T.; MacGregor, J. *Ind. Eng. Chem. Res.* **1998**, *37*, 3660–3669.
- (7) Arzamendi, G.; Asua, J. M. *J. Appl. Polym. Sci.* **1989**, *38*, 2019–2036.
- (8) Vicente, M.; Leiza, J. R.; Asua, J. M. *Chem. Eng. Sci.* **2003**, *58*, 215–222.
- (9) Billmeyer, F. W., Jr. *Textbook of Polymer Science*, 3rd ed.; John Wiley & Sons: Singapore, 1994.
- (10) Krämer, S.; Gesthuisen, R.; Wieland, M.; Engell, S. An Alternative Model Formulation for Emulsion Polymerization Processes. In *Conference Proceedings of the European Congress of Chemical Engineering*; VDI-GVC: Frankfurt, Germany, 2001.
- (11) Urretabizkaia, A.; Leiza, J.; Asua, J. *AIChE J.* **1994**, *40*, 1850–1864.
- (12) Srinivasan, B.; Palanki, S.; Bonvin, D. *Comput. Chem. Eng.* **2003**, *27*, 1–26.
- (13) Gugliotta, L. M.; Arotcarena, M.; Leiza, J. R.; Asua, J. M. *Polymer* **1995**, *36*, 2019–2023.
- (14) Asua, J. M. On-line Control of Emulsion Polymerization Reactors. In *5th International Workshop on Polymer Reaction Engineering*; Reichert, K. H., Ed.; VCH-Verlagsgesellschaft: Berlin, 1995; pp 655–671.
- (15) de Buruaga, I. S.; Echevarria, A.; Armitage, P. D.; de la Cal, J. C.; Leiza, J. R.; Asua, J. M. *AIChE J.* **1997**, *43*, 1069–1081.
- (16) Gelb, A. *Applied Optimal Estimation*; MIT Press: Cambridge, MA, 1974.
- (17) Krämer, S.; Gesthuisen, R.; Engell, S.; Asua, J. M. Simultaneous estimation of heat transfer coefficient and reaction heat in semi-batch processes. In *Conference Proceedings of American Automatic Control Conference 2003*; Bequette, W., Ed.; American Automatic Control Council, IEEE Press: Piscataway, NJ, 2003; pp 1980–1981.
- (18) Tietze, A. Möglichkeiten und Grenzen der Temperaturschwingungskalorimetrie. Ph.D. Thesis, Universität Berlin, Berlin, Germany, 1998.
- (19) Villadsen, J.; Michelsen, M. *Solution of Differential Equation Models by Polynomial Approximation*; Prentice-Hall: Englewood Cliffs, NJ, 1978.
- (20) Krämer, S.; Gesthuisen, R.; Engell, S. Fehlerhafte Schätzung des Wärmeübergangskoeffizienten in Rührkesseln durch Modellvereinfachung. In *GMA-Kongress Automation und Information in Wirtschaft und Gesellschaft*; VDI-Verlag: Düsseldorf, Germany, 2003; Vol. 1756, pp 529–536.
- (21) Gesthuisen, R.; Engell, S. State Estimation for Tubular Reactors with Measurements at the Outlet Only. In *Proceedings of ADCHEM 2000: International Symposium on Advanced Control of Chemical Processes*; Elsevier Science Ltd.: Amsterdam, The Netherlands, 2000; Vol. 2, pp 971–976.
- (22) Gesthuisen, R.; Krämer, S.; Engell, S. State Estimation for Semicontinuous Emulsion Copolymerization Using Calorimetric Data. In *Conference Proceedings of the American Automatic Control Conference*; Krogh, B. H., Ed.; American Automatic Control Council, IEEE Press: Piscataway, NJ, 2001; pp 362–367.

- (23) Dimitratos, Y. N. Modeling and Control of Semicontinuous Emulsion Copolymerization, Ph.D. Thesis, Lehigh University, Bethlehem, PA, 1989.
- (24) Arzamendi, G.; Leiza, J. R.; Asua, J. M. *J. Polym. Sci. A: Polym. Chem.* **1991**, *29*, 1549–1559.
- (25) Li, B.; Brooks, B. W. *J. Polym. Sci. A: Polym. Chem.* **1993**, *31*, 2397–2402.
- (26) Li, B.; Brooks, B. W. *J. Appl. Polym. Sci.* **1993**, *48*, 1811–1823.
- (27) Plessis, C.; Arzamendi, G.; Leiza, J. R.; Schoonbrood, H. A. S.; Charmot, D.; Asua, J. M. *Macromolecules* **2000**, *33*, 5041–5047.
- (28) Forcada, J.; Asua, J. M. *J. Polym. Sci. A: Polym. Chem.* **1990**, *28*, 987–1009.
- (29) Asua, J. M.; Sudol, E. D.; El-Aasser, M. S. *J. Polym. Sci. A: Polym. Chem.* **1989**, *27*, 3903–3913.
- (30) Asua, J. M. *Macromolecules* **2003**.
- (31) Nomura, M.; Harada, M. *J. Appl. Polym. Sci.* **1981**, *26*, 17–26.
- (32) Odian, G. *Principles of Polymerization*; Wiley: New York, 1991.
- (33) Urretabizkaia, A.; Asua, J. M. *J. Polym. Sci. A: Polym. Chem.* **1994**, *32*, 1761–1778.
- (34) Arzamendi, G.; Asua, J. M. *Macromolecules* **1995**, *28*, 7479–7490.
- (35) Elias, H.-G. *Makromoleküle: Band 1 Grundlagen–Struktur, Synthese, Eigenschaften*, 5th ed.; Hüthig & Wepf Verlag: Basel, Switzerland; 1990.

Received for review December 18, 2003

Revised manuscript received September 10, 2004

Accepted September 10, 2004

IE0343263